Glucocorticoids Regulate the Metabolic Hormone FGF21 in a Feed-Forward Loop

Rucha Patel,* Angie L. Bookout,* Lilia Magomedova, Bryn M. Owen, Giulia P. Consiglio, Makoto Shimizu, Yuan Zhang, David J. Mangelsdorf, Steven A. Kliewer, and Carolyn L. Cummins

Department of Pharmaceutical Sciences (R.P., L.M., G.P.C., C.L.C.), University of Toronto, Toronto, Ontario, Canada M5S 3M2; Department of Pharmacology and Howard Hughes Medical Institute (A.L.B., B.M.O., M.S., Y.Z., D.J.M.), and Department of Molecular Biology (S.A.K.), University of Texas Southwestern Medical Center, Dallas, Texas 75390; and Banting and Best Diabetes Centre (C.L.C.), Toronto, Ontario, Canada M5G 2C4

Hormones such as fibroblast growth factor 21 (FGF21) and glucocorticoids (GCs) play crucial roles in coordinating the adaptive starvation response. Here we examine the interplay between these hormones. It was previously shown that FGF21 induces corticosterone levels in mice by acting on the brain. We now show that this induces the expression of genes required for GC synthesis in the adrenal gland. FGF21 also increases corticosterone secretion from the adrenal in response to ACTH. We further show that the relationship between FGF21 and GCs is bidirectional. GCs induce Fgf21 expression in the liver by acting on the GC receptor (GR). The GR binds in a ligand-dependent manner to a noncanonical GR response element located approximately 4.4 kb upstream of the Fgf21 transcription start site. The GR cooperates with the nuclear fatty acid receptor, peroxisome proliferator-activated receptor-α, to stimulate Fgf21 transcription. GR and peroxisome proliferator-activated receptor-α ligands have additive effects on Fgf21 expression both in vivo and in primary cultures of mouse hepatocytes. We conclude that FGF21 and GCs regulate each other's production in a feed-forward loop and suggest that this provides a mechanism for bypassing negative feedback on the hypothalamic-pituitary-adrenal axis to allow sustained gluconeogenesis during starvation. (***Molecular Endocrinology*** **29: 213–223, 2015)**

Fibroblast growth factor (FGF)-21 is a metabolic hormone with physiological relevance to starvation and pharmacological potential for the treatment of obesity. FGF21 levels increase with prolonged fasting in response to rising free fatty acids through the activation of peroxisome proliferator-activated receptor (PPAR)-α in the liver (1, 2). FGF21 circulates in the bloodstream and coordinates a starvation response that includes increasing gluconeogenesis, ketogenesis, and fatty acid oxidation (1–3). Overall, FGF21 acts to coordinate whole-body fat use and energy expenditure. In obese rodents, monkeys, and humans, FGF21 lowers circulating and hepatic triglyceride and cholesterol concentrations, causes weight loss, and improves insulin sensitivity (4, 5).

FGF21 is an atypical member of the FGF superfamily in that it lacks the heparin binding domain characteristic of other FGFs, a feature allowing diffusion away from the tissue in which it is produced. The endocrine actions of FGF21 are mediated through FGF receptors (FGF receptors 1–4) but require the presence of a coreceptor (β-klotho) to elicit a response. Selectivity in the tissues responsive to FGF21 is achieved via the more limited tissue distribution of β-klotho (6–9).

ISSN Print 0888-8809 ISSN Online 1944-9917
Printed in U.S.A.

Received August 14, 2014. Accepted December 8, 2014.
First Published Online December 11, 2014

* R.P. and A.L.B. contributed equally to this work.

Abbreviations: ChIP, chromatin immunoprecipitation; CNS, central nervous system; Ct, cycle threshold; DEX, dexamethasone; DR3, direct repeat 3; DTT, dithiothreitol; FBS, fetal bovine serum; FGF, fibroblast growth factor; GBS, GR binding site; GC, glucocorticoid; GR, GC receptor; H3, histone 3; IR3, inverted repeat 3; MC2R, melanocortin 2 receptor; PPAR, peroxisome proliferator-activated receptor; QPCR, quantitative PCR; StAR, steroidogenic acute regulatory protein; STAT5, signal transducer and activator of transcription 5; TSS, transcription start site; WT, wild type; WY, WY-14643.

Similar to the important role of FGF21 in starvation, glucocorticoids (GCs) are increased under conditions of acute and chronic stress in which glucose must be produced to provide fuel for the brain. The hypothalamic-pituitary-adrenal axis is the primary regulator of systemic GC levels. The acute response to stress is mediated by hypothalamic induction of CRH, acting at the anterior pituitary to release ACTH. ACTH binds to the melanocortin 2 receptor (MC2R) at the adrenal gland, which increases the expression of all genes involved in the synthesis of GCs from cholesterol. GCs are secreted into the bloodstream in which they act on multiple tissues to ensure an adequate supply of carbon precursors for the production of glucose, including the liver in which GCs upregulate the expression of enzymes important in gluconeogenesis. Glucocorticoid signaling is critical for the phenotype of hyperglycemia in the *ob/ob* and *db/db* mouse models of type 2 diabetes that have high circulating GC levels (10–13).

Several lines of evidence suggest that the FGF21 and GC signaling pathways are interconnected including the following: 1) numerous genes induced by FGF21 (ie, *Pgc1α*, *Pepck*, *G6Pc*, *Igfbp*) are also induced by GC treatment; 2) it was previously shown that FGF21 transgenic mice (FGF21-Tg) exhibit osteopenia (14), a condition also caused by excessive GC signaling (15); 3) FGF21-Tg mice were recently shown to have increased circulating GC levels (16); and 4) FGF21 levels are elevated in disease states for which GCs are also elevated (ie, type 2 diabetes and mouse models of obesity, *db/db* and *ob/ob*) (17, 18).

Using a brain-selective deletion of β-klotho, we recently reported that many actions of FGF21 on circadian behavior and metabolism (including the regulation of circulating GC levels) are mediated via FGF21 signaling at the level of the central nervous system (CNS) (16). Herein we further explore the molecular basis for increased corticosterone levels in FGF21-Tg mice and show that FGF21 increases adrenal corticosterone synthetic enzymes and renders adrenal cells hyperresponsive to ACTH. In addition, we demonstrate that the transcriptional regulation of FGF21 is strongly induced by GC receptor (GR) activation and additive with PPARα activation. Together these data support a model whereby GC regulation of FGF21, and conversely, FGF21's regulation of GCs, can circumvent the classic negative feedback of the hypothalamic-pituitary-adrenal axis, allowing the prolonged elevation of FGF21 levels and sustained activation of the gluconeogenic pathway during a long-term fast.

Materials and Methods

Chemicals, proteins, and antibodies

All chemicals were obtained from Sigma unless otherwise stated. The β-actin antibody was obtained from Abcam (ab8227). The steroidogenic acute regulatory protein (StAR) antibody was a gift from D. M. Stocco (Texas Tech University Health Sciences Center, Lubbock, Texas). Recombinant human FGF21 was kindly provided by Moosa Mohammadi (New York University Langone Medical Center, New York, New York). ACTH was purchased from Sigma.

Animal studies

All procedures and use of animals were approved by the Institutional Animal Care and Use Committee of University of Texas Southwestern Medical Center Dallas or the Animal Care Committee of the University of Toronto. All animals were maintained on 2016/2916 Global Diet (Harlan Teklad). Male mice were used in all studies. The generation of the *Fgf21*−/− and FGF21-Tg mice has been described elsewhere (1, 19). For all studies using wild-type mice (WT), the background strain is indicated with each experiment and is 129SvEv, C57Bl/6J, or a 1:1 mixture of these two strains (mixed). *Pparα*$^{-/-}$ (C57Bl/6J) and matching WT mice were maintained in a temperature- and light-controlled environment (12 h light, 12 h dark cycles). WT and *Pparα*$^{-/-}$ mice (C57Bl/6J) were injected with dexamethasone (DEX; 5% EtOH in sesame oil) at 2.5 mg/kg twice a day for 5 days. In a separate experiment WT (129SvEv strain) mice were ip injected with DEX (5 mg/kg) and WY14643 (20 mg/kg) in 10% EtOH in saline alone or in combination at 20 hours and 6 hours prior to the time the animals were killed. Animals were killed at times indicated by rapid decapitation to avoid stress responses. Trunk blood was collected into K^+EDTA tubes, and plasma was separated and stored at −80°C until assayed. Tissues were collected, snap frozen in liquid nitrogen, and stored at −80°C until assayed.

Primary culture of adrenal cells

All adrenals were dissected from mice in the fed state unless otherwise indicated. Adrenals from 10 mice per group were digested as described previously (20). Supernatants of viable cells were pooled and seeded at a density of 150 000 cells/well in 24-well plates and maintained at 37°C, 5% CO_2 in DMEM containing 100 U/mL penicillin and 100 μg/mL streptomycin supplemented with 2.5% fetal calf serum, 2.5% horse serum, and 1% insulin/transferrin/selenium (Sigma-Aldrich) for 2 days. On the third day, cells were placed in serum-free media for 24–48 hours. Media were then stored at −80°C until directly assayed by a RIA.

RNA isolation, cDNA synthesis, and real-time quantitative PCR (QPCR) analysis

Total RNA was extracted from tissues using STAT-60 (Tel-Test, Inc), treated with deoxyribonuclease I (RNase-free; Roche), and reverse transcribed using the high-capacity cDNA kit (Applied Biosystems Inc). Human adrenal and human adipose RNA was obtained from Ambion. H295R cell RNA and Y1 cell RNA were obtained from experiments described elsewhere (21). Gene expression profiles were measured by QPCR

(ABI7900) using the ΔΔ cycle threshold (Ct) assay as previously described (22). Primers are available on request.

Plasma analyses

Glucose, ketones, cholesterol, nonesterified fatty acids, and triglycerides were measured by colorimetric assays (Wako); corticosterone (^{3}H) and ACTH (^{125}I) by RIA (MP Biomedical); and FGF21 by ELISA (Biovendor) according to the manufacturers' instructions (16, 21, 23).

Western blot analysis

A single adrenal gland was dounce homogenized 25 times in hypotonic buffer [250 mM sucrose; 10 mM HEPES, pH 7.4; 1 mM EDTA; 2 mM dithiothreitol (DTT); 1 mM phenylmethylsulfonyl fluoride; and protease inhibitors (Complete, Roche)] on ice. The homogenate was centrifuged at 1000 × *g* for 10 minutes, and the supernatant was saved as the cytosolic fraction. Protein concentration was measured using Bradford assay (Bio-Rad Laboratories), and 20 μg of protein extract was loaded on a 12% SDS-PAGE and then transferred onto polyvinyl difluoride membrane. Membranes were incubated overnight at 4°C with primary polyclonal antibodies against StAR (1:1000) or β-actin (1:1000) followed by a 1-hour incubation with a peroxidase-conjugated antirabbit IgG (1:2000). Peroxidase activity was measured using ECL Plus (GE Healthcare) and visualized using the Storm phosphorimager (GE Healthcare). Quantitation was performed using ImageQuant from GE Healthcare.

Primary hepatocyte isolation

Primary hepatocytes were isolated from WT mice by collagenase perfusion and purified by centrifugation as described (24). In brief, mouse liver was first perfused with liver perfusion medium (Invitrogen) for 10 minutes followed by liver digestion medium for 10 minutes at the flow rate of 3 mL/min using a peristaltic pump (GE Healthcare). Freshly prepared hepatocytes were seeded at a final density of 0.5×10^6 cells/well onto type I collagen coated six-well plates in attachment media [William's E media, 10% charcoal stripped fetal bovine serum (FBS), 1× penicillin/streptomycin, and 10 nM insulin]. Media were exchanged 2 hours after plating, and all the experiments were performed on the second day. Ligands were added to the cells in M199 media without FBS and cells were harvested 9 hours after ligand treatment for RNA extraction.

Chromatin immunoprecipitation (ChIP)

ChIP was carried out using the EZ ChIP kit (Millipore). Livers were perfused in situ for 30 minutes via the portal vein with either vehicle or 10 nM DEX. Whole liver was minced and cross-linked in 1% formaldehyde containing PBS, 1 mM DTT, and 1 mM phenylmethylsulfonyl fluoride for 10 minutes at room temperature. Cross-linking was stopped by addition of glycine to final concentration of 125 mM for 5 minutes at room temperature, followed by centrifugation and washing the pellet twice in ice-cold PBS containing 1 mM DTT and protease inhibitors (Complete; Roche). Liver nuclei were recovered by dounce homogenization in a hypotonic buffer [10 mM HEPES (pH 7.9), 1.5 mM $MgCl_2$, 10 mM KCl, 0.2% Nonidet P-40, 0.2 mM sodium orthovanadate, 0.15 mM spermine, 0.5 mM spermidine, 1 mM EDTA, 5% sucrose, 1 mM DTT, and protease inhibitors] and layered onto a cushion buffer [10 mM Tris-HCl (pH 7.5), 15 mM NaCl, 60 mM KCl, 0.15 mM spermine, 0.5 mM spermidine, 1 mM EDTA, 10% sucrose, 1 mM DTT, and protease inhibitor] followed by centrifugation. The nuclei pellet was washed with cold PBS and resuspended in 2 mL sonication buffer [0.75% sodium dodecyl sulfate, 2 mM EDTA, and 50 mM Tris-HCl (pH 8.0)]. The chromatin was sheared to 200–1000 bp by sonication. The sonicated chromatin was diluted 7.5-fold in dilution buffer (Millipore), and 800 μL of diluted sample per immunoprecipitation was used. After 1 hour preclearing with protein G-agarose beads (100 μL, ip), 10 μg of GR (M-20) antibody (Santa Cruz Biotechnology, Inc) was added for overnight incubation. Protein G agarose (50 μL) was used to recover the immune complexes (2 h at 4°C).

Washes and elutions were performed in accordance with the ChIP kit. DNA was reverse cross-linked overnight at 65°C, RNAase treated for 30 minutes at 37°C, and proteinase K treated for 2 hours at 45°C and purified using a spin column to a final volume of 50 μL. The eluate was diluted 5-fold with water, and QPCR was performed in triplicates using 5 μL of template DNA with the following primers listed in Supplemental Table 1. Quantitation was performed by QPCR (standard curve method) using serial dilutions of the input as standards.

FGF21 reporter constructs and primary hepatocyte luciferase reporter assays

The pGL4.10-E4TATA was from Dr Eric Bolton (University of Illinois at Urbana-Champaign, Urbana, Illinois). Specific mouse Fgf21 promoter regions were amplified from genomic mouse DNA using Platinum Taq high-fidelity DNA polymerase (Invitrogen) and cloned into the pGL4.10-E4TATA vector using *Kpn*I and *Xho*I sites. Promoter deletion and mutant constructs were generated using a QuikChange site-directed mutagenesis kit (Agilent). Oligonucleotides with three copies of the putative GR binding sites (GBSs), and the corresponding mutants were synthesized with *Kpn*I-*Xho*I sites (see Supplemental Table 2 for oligonucleotide sequences). Annealed oligonucleotides were then cloned into the pGL4.10-E4TATA vector.

For FGF21 gene reporter activation assays, the primary hepatocytes were transfected using Lipofectamine 2000 (Invitrogen) in OPTI-MEM media. The total amount of plasmid DNA (250 ng/well) included 125 ng FGF21 gene fragment reporter plasmids, 50 ng *Renilla* plasmid, 25 ng pCMX-mGR plasmid, and 50 ng filler CMX plasmid. Six hours after transfection, the media were changed to M199 media supplemented with 10% super stripped FBS, 1 nM insulin and 100 U/mL penicillin/100 μg/mL streptomycin. The next evening, ligands were added in M199 media (without FBS). Cells were harvested 20 hours later in passive lysis buffer (Promega), and luciferase and *Renilla* activities were measured using a dual-luciferase kit (Promega). Luciferase values were normalized to *Renilla* to control for transfection efficiency and expressed as relative luciferase units.

Statistics

Data are presented as mean ± SEM. GraphPad Prism was used for ANOVA followed by multiple comparisons testing as appropriate or by a two-tailed Student's *t* test. $P < .05$ was considered significant.

Results

Adrenal corticosterone production is increased in FGF21-Tg mice but is not the result of direct action of FGF21 on adrenocortical cells

We recently reported that circulating corticosterone levels were increased in both FGF21-Tg mice and WT mice administered recombinant FGF21 at fasting levels via osmotic minipump (16). Surprisingly, however, plasma ACTH levels were reduced in both the FGF21-Tg mice and mice administered FGF21. In an effort to understand how FGF21 increases corticosterone levels, we examined adrenals from WT and FGF21-Tg mice. As expected, we observed a 3.6-fold increase in circulating corticosterone levels in FGF21-Tg compared with WT mice (Figure 1A). Concurrently, circulating ACTH levels were suppressed 10-fold in FGF21-Tg mice compared with WT mice (Figure 1B). Interestingly, we found that the adrenal weights of FGF21-Tg mice were 1.6-fold heavier than WT mice when normalized to body weight (0.040 ± 0.002 vs 0.068 ± 0.006 g/g%; WT vs FGF21-Tg, $P < .05$). By histology, we were able to confirm that FGF21-Tg mice had increased cellularity in the cortex indicating increased adrenal mass is due to hyperplasia. Furthermore, we noted that the cholesterol ester-rich lipid droplets (measured by Oil red O) were diminished in the cortical cells of FGF21-Tg adrenal glands, in line with the enhanced glucocorticoid production observed in these mice (Supplemental Figure 1, A and B). These findings suggest that FGF21 causes an ACTH-independent adrenomegaly.

We next examined corticosterone secretion from primary cultures of adrenal cells prepared from WT and FGF21-Tg mice. Notably, during primary cell isolation we found that the number of adrenal cells obtained from FGF21-Tg mice was consistently higher than that obtained from WT mice, supporting the hypothesis that adrenal hyperplasia accounts at least in part for the observed adrenomegaly. We accounted for this difference by plating equal cell numbers and confirming that the results were not altered when normalized for DNA content of each well (data not shown). Primary adrenal cells from FGF21-Tg mice exhibited significantly increased corticosterone secretion relative to WT mice, under both basal and ACTH stimulation (Figure 1C). Together these data support the idea that, in the whole animal, FGF21 stimulates adrenal production of corticosterone and sensitizes the adrenal response to ACTH.

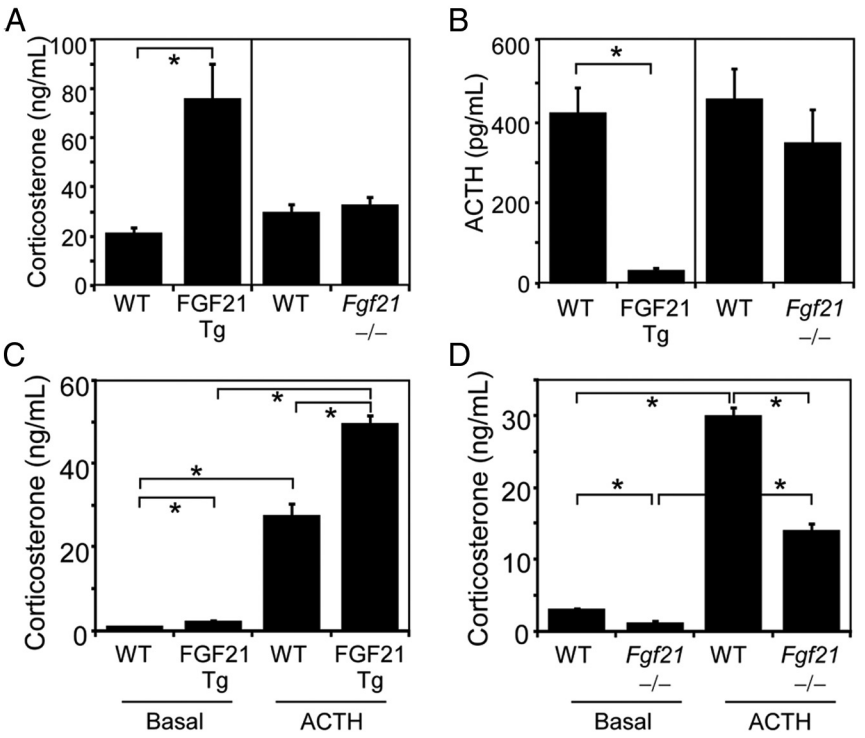

Figure 1. FGF21 transgenic mice are hypercorticosteronemic. Circulating plasma corticosterone (A) and ACTH levels (B) were measured in FGF21-Tg (3–4 mo old, C57Bl/6J) and *Fgf21*$^{-/-}$ mice (5–8 mo old, mixed strain) along with their respective controls (WT). Mice were sacrificed at lights on when endogenous GC levels are at the nadir ($n \geq 8$). C and D, Corticosterone secretion from primary cultures of adrenal cells from 3-month-old WT, FGF21-Tg, and *Fgf21*$^{-/-}$ mice (C57BL/6J) incubated with vehicle or 15 ng/mL ACTH for 48 hours. Data in panels C and D shown as average ± SEM ($n = 5–6$ independent samples from ~10 pooled adrenals per genotype). *, $P < .05$ relative to WT group (ANOVA followed by Student-Newman-Keuls).

In complementary experiments, we examined corticosterone secretion from the adrenals of *Fgf21*−/− mice. No significant differences in basal corticosterone or ACTH were observed in *Fgf21*−/− mice compared with WT mice (Figure 1, A and B). However, in primary adrenal cells derived from young (3 mo old) *Fgf21*−/− mice, we observed decreased secretion of corticosterone relative to WT mice, under basal and ACTH-stimulated conditions (Figure 1D). These data suggest that FGF21 expression per se is not strictly required for basal maintenance of GC levels in vivo but does affect basal adrenal responsiveness to ACTH.

FGF21-Tg mice have increased adrenal steroid synthetic enzymes

To determine whether FGF21 directly activates GC synthesis at the level of the adrenal gland, we incubated primary adrenal cells with recombinant FGF21 (with and with-

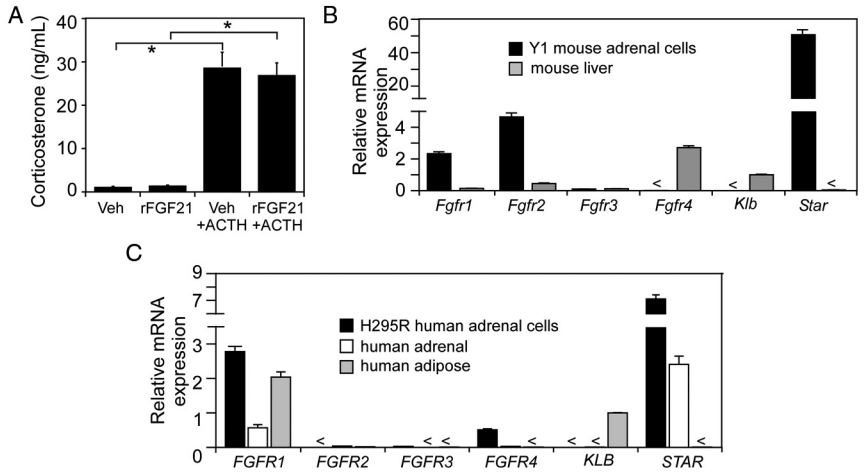

Figure 2. FGF21 indirectly promotes the sensitization of adrenocortical cells to ACTH. A, Primary adrenal cultures from C57BL/6J WT mice were plated and treated in culture with recombinant FGF21 (0.5 μg/mL) and/or ACTH (15 ng/mL) for 24 hours. Corticosterone secreted in the media was measured by a RIA (average ± SEM; n = 5–6 independent samples from ~10 pooled adrenals). *, $P < .05$ relative to WT group (ANOVA followed by Student Newman Keuls). rFGF21, rat FGF21. B, QPCR expression of the FGFs, β-klotho coreceptor (*Klb*), and *Star* in the mouse adrenal cortical cell line Y1 compared with mouse liver expression levels. C, QPCR expression of the FGF receptors, β-klotho (*KLB*) and *STAR*, in the human adrenal cortical cell line H295R and human adrenal gland RNA compared with human adipose RNA. Data in panels B and C are normalized to 18S and expressed relative to β-klotho (set to 1) and shown as the average ± SD of the variation in the real-time QPCR reaction (n = 3). < signifies the samples were run but the signal was below the limit of detection.

out added ACTH) and measured corticosterone secretion. No increase in corticosterone secretion was seen with the addition of recombinant FGF21, suggesting that the effect of FGF21 on plasma corticosterone levels is indirect (Figure 2A). The lack of direct activation of the adrenal gland by FGF21 is also in agreement with the very low expression of β-klotho mRNA in mouse and human adrenal glands and adrenal-derived cell lines (Figure 2, B and C). Our recently published data showing that a CNS-selective β-klotho knockout reverses the phenotype of hypercorticosteronemia in FGF21-Tg mice further supports that FGF21 acts via the CNS to modulate GC production (16).

We compared the expression of genes important in adrenal steroid synthesis in WT, FGF21-Tg, and *Fgf21*−/− mice. The rate-limiting enzyme in GC production is the StAR, which transfers cholesterol from the outer to the inner mitochondrial membrane. Cytochrome P450 11a1 (Cyp11a1) and 3β-hydroxy-δ5-steroid dehydrogenase (Hsd3b1) are both important for the conversion of cholesterol to GCs; steroidogenic factor-1 (Sf1) is important in maintaining the basal expression of the steroidogenic genes; and the melanocortin 2 receptor (Mc2r) is the receptor for ACTH. A significant increase in the basal expression of Sf1, Mc2r, Cyp11a1, and Hsd3b1 was observed in FGF21-Tg mice compared with WT mice (Figure 3A). No significant change in any of the genes was observed in the *Fgf21*−/− mice compared with WT mice (Figure 3B). Although the mRNA expression of StAR in FGF21-Tg followed the same trend as other genes, it did not reach statistical significance. However, at the protein level, StAR was increased 2-fold compared with WT mice (Figure 3C).

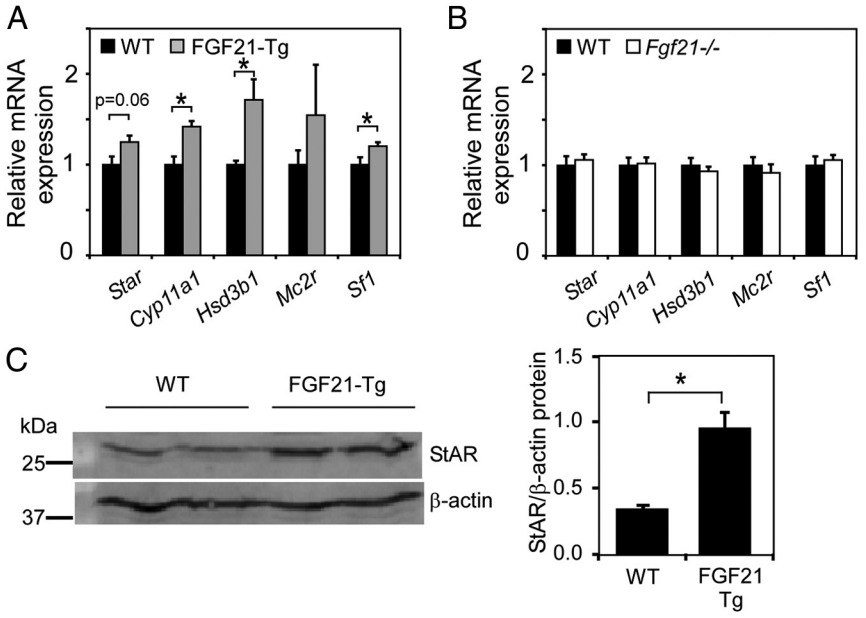

Figure 3. FGF21-Tg mice have elevated basal expression of steroidogenic genes compared with WT mice. A and B, Adrenal mRNA expression of Star, Cyp11a1, Hsd3b1, Mc2r, and Sf1 was measured by QPCR in FGF21-Tg and *Fgf21*$^{-/-}$ mice (samples obtained at lights off, n = 4). Samples were normalized to the mRNA expression of 18S. C, Western blot of adrenal protein lysates (20 μg) from WT and FGF21-Tg mice (killed 4 h after lights on) blotted for StAR (30 kDa) and β-actin (42 kDa). Protein quantitation is represented normalized to β-actin. *, $P < .05$ relative to WT control (Student's *t* test).

To determine whether increased adrenal enzyme production would be observed in the presence of physiological concentrations of FGF21, we analyzed the adrenal glands from mice receiving 1.1 μg/h of recombi-

nant FGF21 via sc implanted Alzet minipump for 7 days (16). In agreement with our previous report showing enhanced corticosterone levels in WT mice receiving FGF21 (16), recombinant administration of FGF21 increased adrenal Cyp11a1 expression significantly and showed a tendency to increase the levels of other important steroidogenic factors Hsd3b1, Mc2r, and Sf1 (Supplemental Figure 2). Notably, these trends were not observed when recombinant FGF21 was dosed to mice lacking β-klotho expression in the CNS (Supplemental Figure 2), consistent with the idea that FGF21 mediates this response indirectly through the brain.

GCs induce Fgf21 expression

Given the relationship between FGF21 and corticosterone, we next examined whether GCs, which are induced by fasting, might themselves regulate Fgf21 expression. To test this in vivo, we treated WT and *Pparα*$^{-/-}$ mice with the potent, selective synthetic GC DEX (5 d treatment). *Pparα*$^{-/-}$ mice were included in this experiment due to the prominent role PPARα plays in inducing Fgf21 in response to fasting. Notably, liver Fgf21 levels were increased 7-fold with DEX compared with vehicle in WT mice. Similarly, *Ppar[alpha]*$^{-/-}$ mice showed a significant induction with DEX (12-fold), but the absolute level of FGF21 remained below that of the WT vehicle-treated mice (Figure 4A). The significantly different baseline levels of FGF21 in WT vs *Pparα*$^{-/-}$ mice (WT chow: Ct = 27.5; *Pparα*$^{-/-}$ chow: Ct = 32; Figure 4A) are in agreement with previously published data showing that PPARα is required for maintaining basal FGF21 expression (1, 2). The induction of FGF21 by DEX was also seen at the protein level with a 15-fold increase in circulating FGF21 in DEX-treated vs vehicle-treated WT mice (Figure 4B). Consistent with the lower gene expression levels of FGF21 in the *Pparα*$^{-/-}$ mice, we were unable to detect FGF21 in the plasma of *Pparα*$^{-/-}$ vehicle-treated animals (Figure 4B).

To assess whether GCs activate FGF21 directly at the level of the liver and not through altered signaling from other tissues, we performed experiments in mouse primary hepatocytes. Treatment of hepatocytes with DEX increased FGF21 levels 3-fold (Figure 4C). This was attributed to the actions of the GR because cotreatment of DEX with RU486 eliminated this response (Figure 4C). Consistent with a direct role of GR in mediating FGF21 induction, treatment with the protein synthesis inhibitor cycloheximide did not affect the GR's ability to induce FGF21 (Figure 4D). Thus, our studies in primary hepatocytes show that GCs act directly on GR in liver to induce Fgf21 expression.

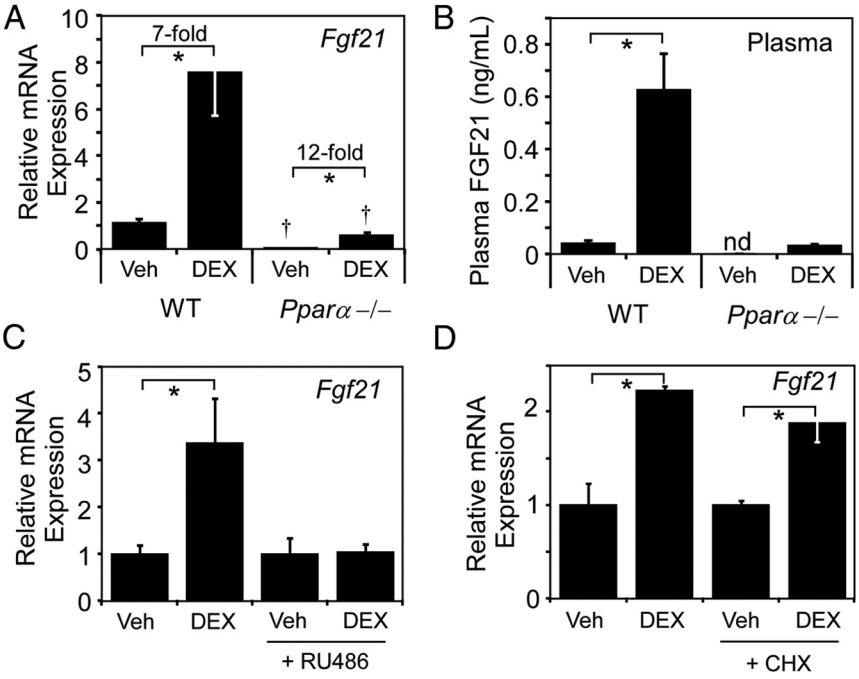

Figure 4. Hepatic FGF21 is induced by GR activation in a cell-autonomous manner. A, Liver gene expression of Fgf21 after DEX treatment (sc injection 2.5 mg/kg twice a day, 5 d) in WT and *Pparα*$^{-/-}$ mice. Mice were killed at lights on. Vehicle-treated Ct values were 27.5 for WT and 32 for *Pparα*$^{-/-}$. Veh, vehicle. B, Plasma levels of FGF21 from matching mouse samples measured by ELISA. Data shown represent average ± SEM (n = 4–6). C and D, Primary hepatocytes from WT mice (129SvEv) were treated with indicated ligands for 9 hours. C, QPCR analysis of Fgf21 expression after treatment with DEX (100 nM) ± the GR antagonist RU486 (1 μM). D, QPCR analysis of Fgf21 expression after treatment with DEX (100 nM) ± cycloheximide (CHX; 5 μM), normalized to cyclophilin. Data shown represent average ± SD (n = 3). *, $P < .05$ relative to vehicle control (ANOVA followed by Student-Newman-Keuls).

GCs activate FGF21 expression via a noncanonical GR binding site 4.4 kb downstream of the transcription start site (TSS)

To confirm that GR was indeed acting directly at the *Fgf21* gene locus, we performed a promoter walking analysis using ChIP. Livers of WT mice were perfused in situ with either vehicle or 10 nM DEX for 30 minutes. After perfusion, the livers were fixed and processed for ChIP using an antibody selective for GR. Using primers at approximately 1-kb intervals along the length of the gene (from −10 kb to +10 kb surrounding the TSS), we determined that GR was selectively recruited in a ligand-dependent manner to at least two regions that were approximately −1 kb and +5 kb from the

FGF21 transcription start site (Figure 5A). Given that GR binding was detected at +5 kb, outside the FGF21 promoter, we next examined whether this region was in an open chromatin conformation by performing a ChIP against H3K27 acetylation and normalizing these results to the total histone 3 (H3) content. There was significantly more H3K27 acetylation at −1 kb and +5 kb compared with the negative control region at −2.9 kb, demonstrating that these regions are in an open conformation (Figure 5B). Because GR binding in mouse liver is known to favor regions of open chromatin and H3K27 acetylation is a marker of active enhancers, it was not surprising that DEX treatment did not further increase H3K27 acetylation relative to vehicle treatment. However, H3K27 acetylation at the −1 kb site appeared to decrease after DEX treatment. We are unclear of the importance of this observation because the level of H3K27 acetylation remaining was still well above the levels observed at the negative control region (−2.9 kb).

To assess whether the putative GR binding site in the FGF21 promoter was responsible for DEX induction, we performed cotransfection assays in CV-1 cells using a −1.4 kb FGF21 promoter luciferase construct that was previously reported to be PPARα responsive (1). We confirmed PPARα-mediated activation of this reporter; however, we saw no significant change in reporter activation when cells were cotransfected with GR and treated with DEX (data not shown). Using nuclear receptor binding site prediction software [NUBIscan (25)], we found that the region between +4 kb and +5 kb of the FGF21 gene contained two high scoring putative nuclear receptor binding sites. We hypothesized that either the direct repeat 3 (DR3) element (GGAACActcAGGACA) located between +4388 bp and +4374 bp or the inverted repeat 4 element (TGTACAaatgTGTACA) located between +4721 bp and +4705 bp could be atypical GBSs. We subcloned this genomic region (+4.8 kb to +4.3 kb) into an enhancer trap pGL4.10-E4TATA vector plasmid. In transient transfections of mouse primary hepatocytes, deletion or mutation of the DR3, but not the inverted repeat 4, markedly reduced the ability of DEX to stimulate *Fgf21* gene reporter activity (Figure 6A). To establish whether this novel GBS was sufficient to induce GR activation, we cloned three repeating units of the DR3 GBS upstream of the E4TATA promoter. DEX treatment of transiently transfected hepatocytes with the WT 3xGBS construct showed a 51-fold induction in luciferase activity compared with vehicle-treated cells (Figure 6B). In contrast, all of the mutated 3xGBS constructs had significantly attenuated responses to DEX (Figure 6B). These findings indicate that ligand-bound GR activates *Fgf21* gene transcription by binding to an atypical DR3 binding site located approximately 4.4 kb downstream of the TSS.

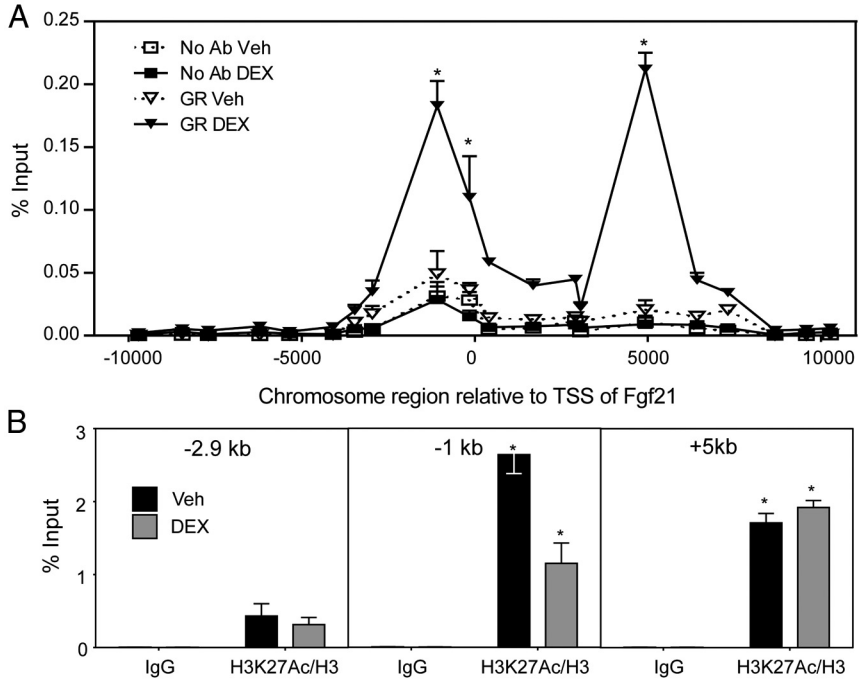

Figure 5. GR binds to two regions of open chromatin surrounding the Fgf21 gene locus. A, ChIP assay demonstrating GR recruitment to the Fgf21 gene locus at −1 kb and +5 kb relative to the TSS (0 kb) after DEX treatment. *, $P < .05$ compared with GR vehicle. B, Acetylation of H3K27 relative to total H3 content at −2.9 kb (negative control region), −1 kb, and +5 kb from the TSS of mFgf21 gene was assessed by real-time QPCR. Data are from a representative experiment (average ± SD, n = 3) repeated in independent sample sets at least three times. *, $P < .05$ compared with the level of H3K27Ac/H3 at −2.9 kb (one way ANOVA followed by Student-Newman-Keuls). Veh, vehicle; Ab, antibody.

GCs act in concert with PPARα to induce FGF21 expression

To determine the individual contribution of GR and PPARα to FGF21 expression, we treated mouse primary hepatocytes with either DEX or the synthetic PPARα agonist WY-14643 (WY). Treatment with saturating doses of DEX (100 nM) or WY (1 μM) alone resulted in a similar level of Fgf21 induction (4- to 5-fold); however, cotreatment with DEX + WY resulted in a 20-fold induction of FGF21 (Figure 7A). To determine whether a similar response occurs in vivo, WT mice were injected with DEX or WY alone or in combination and analyzed the following day for FGF21 gene and protein expression. He-

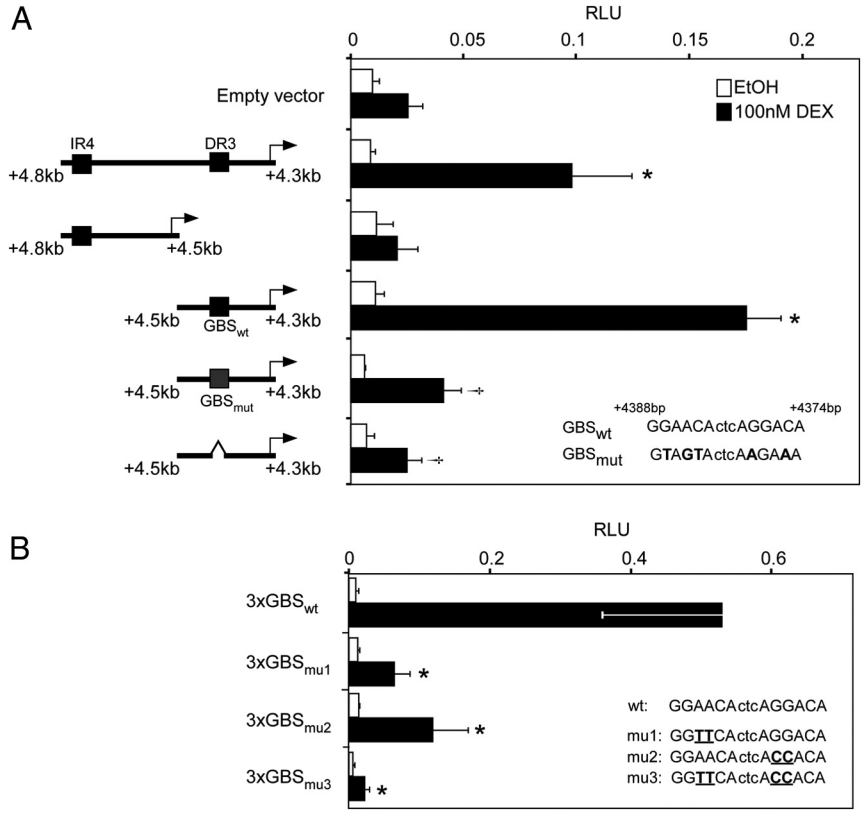

Figure 6. GR activates transcription via an atypical GR binding site 4.4 kb downstream of the Fgf21 TSS. A, Mouse primary hepatocytes were transiently transfected with a series of plasmids containing fragments of the mouse *Fgf21* gene harboring a putative GBS, deleted GBS, or mutated GBS near the *Fgf21* gene locus linked to a luciferase reporter along with mouse GR. Twenty-four hours after transfection, cells were treated with 100 nM DEX for 18 hours and FGF21 GBS activity was measured using the dual-luciferase reporter kit (Promega). Left panel, The constructs used in these experiments are shown. In truncation studies of the *Fgf21* gene fragment reporter, black boxes represent potential GBS sites, gray box represents mutated GBS (sequence shown), and broken lines denotes the construct with putative GBS deleted. B, In mutation studies of 3xGBS reporters, mu1, mu2 and mu3 are different site mutations (sequences shown) of the Fgf21 gene GBS between (+4388 bp and +4374 bp). Data are from a representative experiment average ± SD (n = 3, repeated at least three times). *, $P < .05$ Comparison of vehicle vs DEX; †, $P < .05$, comparison of WT vs mutant or deleted GBS by one-way ANOVA followed by Student-Newman-Keuls.

patic Fgf21 expression was induced 7-fold by DEX or WY treatment alone. Notably, Fgf21 expression increased in an additive (15-fold) manner when the mice were cotreated with DEX and WY (Figure 7B). Moreover, in parallel with the gene expression data, plasma FGF21 levels were elevated in an additive manner after DEX and WY cotreatment (Figure 7C).

Discussion

In the present study, we demonstrate that chronically elevated FGF21 levels increase corticosterone production by inducing the expression of enzymes important for adrenal steroidogenesis. The adrenal steroidogenic effects of FGF21 are mediated indirectly, via the CNS, and appear to increase adrenal responsiveness to ACTH. Conversely, we also discovered a novel feed-forward mechanism whereby GCs themselves upregulate the mRNA expression and protein levels of FGF21. We postulate that this type of feed-forward loop is important for survival under conditions of prolonged fasting or starvation because it provides a mechanism to circumvent the negative feedback regulation of the hypothalamic-pituitary-adrenal axis by GCs and allows sustained activation of gluconeogenesis (Figure 8).

We previously showed that CRH is elevated in the hypothalamus of FGF21-Tg mice (16). In a more recent study (26), it was shown that intracerebroventricular administration of FGF21 induced CRH mRNA via activation of ERK and cAMP response element-binding protein and that induction of GCs and gluconeogenic gene expression by starvation was attenuated in *Fgf21*$^{-/-}$ mice. These studies indicate that FGF21 increases circulating GC concentrations via the up-regulation of CRH. However, there appears to be a second, complementary mechanism. It is well documented that under conditions of prolonged food restriction or starvation, the adrenal gland becomes hyperresponsive to ACTH. For example, in rats subjected to 7 days of starvation, corticosterone levels remained elevated despite a marked decrease in circulating ACTH (27). Similarly, the chronic exposure of mice to FGF21 reduces ACTH levels at the same time that it increases GC concentrations, suggesting that FGF21 sensitizes the adrenal cortex to ACTH. Consistent with this possibility, we now show that primary adrenal cells from FGF21-Tg mice secrete more GCs in response to ACTH than cells derived from WT mice. Interestingly, the sensitivity of the adrenal to ACTH is regulated independently of CRH by the splanchnic nerve (28, 29). Given our recent finding that FGF21 acts on the hypothalamus to stimulate sympathetic nervous system output to brown adipose tissue (30), we speculate that FGF21 also increases sympathetic outflow to the adrenal, thereby increasing ACTH sensitivity and corticosterone release.

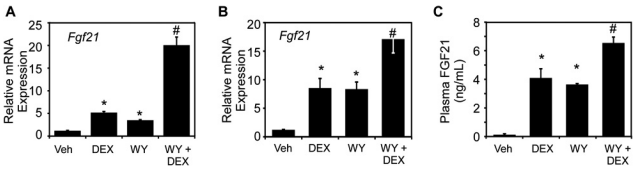

Figure 7. FGF21 expression is induced by DEX and additive with PPARα activation in mice. A, Primary mouse hepatocytes were treated with 1 μM of the PPARα agonist WY or DEX (100 nM) alone or in combination. Fgf21 expression was measured by QPCR with values normalized to cyclophilin (average ± SD, n = 3). B and C, WT mice were administered vehicle (Veh), DEX (5 mg/kg), or WY (20 mg/kg) alone or in combination twice at 20 hours and 6 hours prior to the animals being killed. B, Liver *Fgf21* gene expression measured by QPCR. C, Plasma FGF21 levels were measured by ELISA. In panels B and C, data represent the average ± SEM (n = 4–6). *, $P < .05$, comparison of Veh vs DEX or WY; #, $P < .05$ comparison of DEX vs DEX + WY by one-way ANOVA followed by Student-Newman-Keuls. RLU, relative luciferase unit.

Thus, FGF21 regulates circulating GC levels via a bimodal mechanism.

We show that the induction of FGF21 gene expression and secretion by GCs is mediated by the GR. The GR binds directly to the *Fgf21* gene at a site distinct from that of PPARα and results in an additive effect on FGF21 expression when the ligands for both receptors are present. Cotransfection studies of truncated and mutated FGF21 gene reporters showed that GR binds to the nucleotide sequence GGAACActcAGGACA located +4.4 kb downstream of the FGF21 transcription start site. This GR-regulatory sequence is atypical, in that it is not an inverted repeat 3 (IR3) but is instead a DR3. However, the key central nucleotides in the response element (xGxACAxxxAGAxCx) have previously been shown to be overrepresented in ChIP-sequence studies performed with GR (31). Careful inspection of these conserved residues in the FGF21 GR binding site reveal that the DR3 and IR3 sequences could both satisfy this core requirement for GR binding. This possibility is also supported by the fact that the androgen receptor, another steroid hormone receptor that preferentially binds IR3 sequences, has also been previously shown to bind to a nonconsensus DR3 site (32).

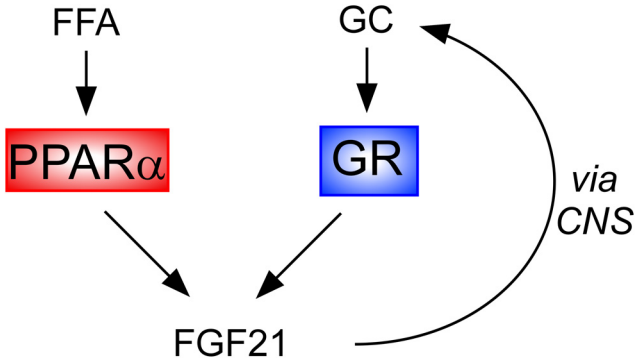

Figure 8. Model for the feed-forward regulation of GCs and FGF21. GCs synergize with PPARα ligands to increase the expression of liver Fgf21. FGF21 is secreted and acts centrally to enhance steroidogenic gene expression in the adrenal gland to increase GC production. FGF21 sensitizes adrenocortical cells to respond to ACTH, despite intact negative feedback of GCs on pituitary ACTH, thus providing an ACTH-independent mechanism to promote prolonged GC synthesis under conditions of chronic stress (including starvation).

The levels of numerous endocrine hormones are altered in response to prolonged fasting to effectively manage the crucial transition between the fed and fasted state (eg, insulin, leptin, ghrelin, glucagon, glucocorticoids, GH, and FGF21). There is a high degree of overlap in the functions of these hormones, which we perceive as a natural built-in redundancy to ensure survival of the organism through prolonged periods of nutrient deprivation (27, 33–36). With this objective in mind, it makes intuitive sense that GCs and FGF21, which are both elevated in the long-term response to fasting and positively regulate gluconeogenesis, feed-forward regulate each other's synthesis. Hormones that are elevated earlier in the fasting response, such as glucagon and GH, have also been shown to increase FGF21 expression. Although glucagon induces FGF21 via activation of AMP-activated protein kinase and PPARα (37), GH has been shown to regulate hepatic FGF21 expression both directly by activating signal transducer and activator of transcription 5 (STAT5) in the liver (38) and indirectly by inducing lipolysis in the adipose (39). The apparent cooperativity in the continuum of endocrine hormones involved in the up-regulation of FGF21 supports a pivotal role for this factor in a broad physiological context. Indeed, FGF21 has recently been implicated in modulating growth and reproduction, two key physiological functions that are repressed with starvation. Although GH normally activates STAT5 in the liver to increase the levels of IGF-1 in circulation, under conditions of prolonged fasting, IGF-1 levels are decreased because FGF21 signaling interferes with STAT5 activation (40). In reproduction, FGF21 was shown to inhibit the LH surge required for ovulation by inhibiting the vasopressin-kisspeptin axis in the suprachiasmatic nucleus (41). Upon nutrient availability, a postprandial increase in insulin promotes the recruitment of the transcriptional repressor E4-binding protein 4to the FGF21 promoter and represses FGF21 gene expression (42).

In addition to the data reported in our study, there are several lines of evidence that support a role of GCs in the regulation of FGF21. A clinical study of patients with Cushing's syndrome, a condition of elevated endogenous glucocorticoids, had elevated FGF21 levels; however, FGF21 levels were not linearly correlated with circulating cortisol levels in these patients (43). Mice treated with the synthetic GC prednisolone for 7 days were found to have a 2-fold increase in FGF21 levels compared with vehicle-treated mice (44). Consistent with a role for glucocorti-

coids in modulating the inducible levels of FGF21, human circadian studies have demonstrated that FGF21 is temporally regulated, with the highest levels appearing in the early morning (45, 46). This pattern correlates tightly with the 24-hour oscillatory pattern of free fatty acids and cortisol (45, 47). Based on our primary hepatocyte and in vivo mouse experiments, the coincident increase in these metabolic regulators of PPARα and GR are likely to both contribute to diurnal FGF21 expression. It will be important to determine using human hepatocytes whether a similar GR binding site is present in the human gene. We were not able to identify a similar glucocorticoid response element in the same region of the human FGF21 locus due to the low level of sequence conservation in this region of the genome.

Our results support a model whereby increased GC signaling induces FGF21, which, in turn, feeds forward to increase GC production. Given this model, we hypothesized that one explanation for the paradoxical finding that genetically obese mice have high circulating FGF21 levels may be their high circulating and/or intratissue corticosterone levels (12, 13, 48, 49). Because humans with insulin resistance and fatty liver are also thought to have enhanced intratissue GC signaling (50, 51), we further speculate that this novel regulatory mechanism may be contributing to the elevated FGF21 levels in these patients (52–54).

Acknowledgments

We gratefully acknowledge Tingting Li (University of Texas Southwestern Medical Center) for help with the 129 primary hepatocyte experiments.

Address all correspondence and requests for reprints to: Carolyn L. Cummins, PhD, Leslie Dan Faculty of Pharmacy, University of Toronto, 144 College Street, Room 1101, Toronto, ON, Canada M5S 3M2. E-mail: carolyn.cummins@utoronto.ca.

This work was supported by Natural Sciences and Engineering Research Council Grant RGPIN-356873 (to C.L.C.), the Howard Hughes Medical Institute (to D.J.M), National Institutes of Health Grant T32-GM007062 (to A.L.B.) and Grant 1RL1GM084436–01 (to S.A.K. and D.J.M.), and the Robert A. Welch Foundation Grant I-1558 (to S.A.K.,) and Grant I-1275 (to D.J.M.).

Current address for M.S.: Department of Applied Biological Chemistry, Graduate School of Agricultural and Life Sciences, The University of Tokyo, Tokyo, Japan.

Disclosure Summary: The authors have nothing to disclose.

References

1. **Inagaki T, Dutchak P, Zhao G, et al.** Endocrine regulation of the fasting response by PPARα-mediated induction of fibroblast growth factor 21. *Cell Metab*. 2007;5(6):415–425.
2. **Badman MK, Pissios P, Kennedy AR, Koukos G, Flier JS, Maratos-Flier E.** Hepatic fibroblast growth factor 21 is regulated by PPARα and is a key mediator of hepatic lipid metabolism in ketotic states. *Cell Metab*. 2007;5(6):426–437.
3. **Potthoff MJ, Inagaki T, Satapati S, et al.** FGF21 induces PGC-1α and regulates carbohydrate and fatty acid metabolism during the adaptive starvation response. *Proc Natl Acad Sci USA*. 2009; 106(26):10853–10858.
4. **Gaich G, Chien JY, Fu H, et al.** The effects of LY2405319, an FGF21 analog, in obese human subjects with type 2 diabetes. *Cell Metab*. 2013;18(3):333–340.
5. **Potthoff MJ, Kliewer SA, Mangelsdorf DJ.** Endocrine fibroblast growth factors 15/19 and 21: from feast to famine. *Genes Dev*. 2012;26(4):312–324.
6. **Kharitonenkov A, Dunbar JD, Bina HA, et al.** FGF-21/FGF-21 receptor interaction and activation is determined by βKlotho. *J Cell Physiol*. 2008;215(1):1–7.
7. **Kurosu H, Choi M, Ogawa Y, et al.** Tissue-specific expression of βKlotho and fibroblast growth factor (FGF) receptor isoforms determines metabolic activity of FGF19 and FGF21. *J Biol Chem*. 2007;282(37):26687–26695.
8. **Ogawa Y, Kurosu H, Yamamoto M, et al.** βKlotho is required for metabolic activity of fibroblast growth factor 21. *Proc Natl Acad Sci USA*. 2007;104(18):7432–7437.
9. **Fon Tacer K, Bookout AL, Ding X, et al.** Research resource: comprehensive expression atlas of the fibroblast growth factor system in adult mouse. *Mol Endocrinol*. 2010;24(10):2050–2064.
10. **Wittmers LE Jr, Haller EW.** Effect of adrenalectomy on the metabolism of glucose in obese (C57 Bl/6J ob/ob) mice. *Metabolism*. 1983;32(12):1093–1100.
11. **Dubuc PU.** Interactions between insulin and glucocorticoids in the maintenance of genetic obesity. *Am J Physiol*. 1992;263(3 Pt 1): E550–E555.
12. **Friedman JE, Sun Y, Ishizuka T, et al.** Phosphoenolpyruvate carboxykinase (GTP) gene transcription and hyperglycemia are regulated by glucocorticoids in genetically obese db/db transgenic mice. *J Biol Chem*. 1997;272(50):31475–31481.
13. **Shimomura Y, Bray GA, Lee M.** Adrenalectomy and steroid treatment in obese (ob/ob) and diabetic (db/db) mice. *Horm Metab Res*. 1987;19(7):295–299.
14. **Wei W, Dutchak PA, Wang X, et al.** Fibroblast growth factor 21 promotes bone loss by potentiating the effects of peroxisome proliferator-activated receptor gamma. *Proc Natl Acad Sci USA*. 2012; 109(8):3143–3148.
15. **Weinstein RS.** Glucocorticoid-induced osteoporosis and osteonecrosis. *Endocrinol Metab Clin North Am*. 2012;41(3):595–611.
16. **Bookout AL, de Groot MH, Owen BM, et al.** FGF21 regulates metabolism and circadian behavior by acting on the nervous system. *Nat Med*. 2013;19(9):1147–1152.
17. **Fisher FM, Chui PC, Antonellis PJ, et al.** Obesity is a fibroblast growth factor 21 (FGF21)-resistant state. *Diabetes*. 59(11):2781–2789.
18. **Hale C, Chen MM, Stanislaus S, et al.** Lack of overt FGF21 resistance in two mouse models of obesity and insulin resistance. *Endocrinology*. 2012;153(1):69–80.
19. **Adams AC, Astapova I, Fisher FM, et al.** Thyroid hormone regulates hepatic expression of fibroblast growth factor 21 in a PPARα-dependent manner. *J Biol Chem*. 285(19):14078–14082.
20. **Patel R, Patel M, Tsai R, et al.** LXRβ is required for glucocorticoid-induced hyperglycemia and hepatosteatosis in mice. *J Clin Invest*. 2011;121(1):431–441.
21. **Cummins CL, Volle DH, Zhang Y, et al.** Liver X receptors regulate adrenal cholesterol balance. *J Clin Invest*. 2006;116(7):1902–1912.
22. **Bookout AL, Cummins CL, Mangelsdorf DJ, Pesola JM, Kramer MF.** High-throughput real-time quantitative reverse transcription PCR. *Curr Protoc Mol Biol*. 2006;Chapter 15:Unit 15.8.

23. **Ding X, Boney-Montoya J, Owen BM, et al.** βKlotho is required for fibroblast growth factor 21 effects on growth and metabolism. *Cell Metab*. 2012;16(3):387–393.
24. **Horton JD, Shimano H, Hamilton RL, Brown MS, Goldstein JL.** Disruption of LDL receptor gene in transgenic SREBP-1a mice unmasks hyperlipidemia resulting from production of lipid-rich VLDL. *J Clin Invest*. 1999;103(7):1067–1076.
25. **Podvinec M, Kaufmann MR, Handschin C, Meyer UA.** NUBIScan, an in silico approach for prediction of nuclear receptor response elements. *Mol Endocrinol*. 2002;16(6):1269–1279.
26. **Liang Q, Zhong L, Zhang J, et al.** FGF21 maintains glucose homeostasis by mediating the crosstalk between liver and brain during prolonged fasting. *Diabetes*. 2014;63(12):4064–4075.
27. **Suemaru S, Hashimoto K, Hattori T, Inoue H, Kageyama J, Ota Z.** Starvation-induced changes in rat brain corticotropin-releasing factor (CRF) and pituitary-adrenocortical response. *Life Sci*. 1986; 39(13):1161–1166.
28. **Edwards AV, Jones CT.** The effect of splanchnic nerve section on the sensitivity of the adrenal cortex to adrenocorticotrophin in the calf. *J Physiol*. 1987;390:23–31.
29. **Engeland WC, Gann DS.** Splanchnic nerve stimulation modulates steroid secretion in hypophysectomized dogs. *Neuroendocrinology*. 1989;50(2):124–131.
30. **Owen BM, Ding X, Morgan DA, et al.** FGF21 acts centrally to induce sympathetic nerve activity, energy expenditure, and weight loss. *Cell Metab*. 2014;20(4):670–677.
31. **Grontved L, John S, Baek S, et al.** C/EBP maintains chromatin accessibility in liver and facilitates glucocorticoid receptor recruitment to steroid response elements. *EMBO J*. 2013;32(11):1568–1583.
32. **Shaffer PL, Jivan A, Dollins DE, Claessens F, Gewirth DT.** Structural basis of androgen receptor binding to selective androgen response elements. *Proc Natl Acad Sci USA*. 2004;101(14):4758–4763.
33. **Makino S, Kaneda T, Nishiyama M, Asaba K, Hashimoto K.** Lack of decrease in hypothalamic and hippocampal glucocorticoid receptor mRNA during starvation. *Neuroendocrinology*. 2001;74(2): 120–128.
34. **van den Berghe G.** The role of the liver in metabolic homeostasis: implications for inborn errors of metabolism. *J Inherit Metab Dis*. 1991;14(4):407–420.
35. **Kersten S, Seydoux J, Peters JM, Gonzalez FJ, Desvergne B, Wahli W.** Peroxisome proliferator-activated receptor α mediates the adaptive response to fasting. *J Clin Invest*. 1999;103(11):1489–1498.
36. **Lemberger T, Saladin R, Vazquez M, et al.** Expression of the peroxisome proliferator-activated receptor α gene is stimulated by stress and follows a diurnal rhythm. *J Biol Chem*. 1996;271(3): 1764–1769.
37. **Berglund ED, Kang L, Lee-Young RS, et al.** Glucagon and lipid interactions in the regulation of hepatic AMPK signaling and expression of PPARα and FGF21 transcripts in vivo. *Am J Physiol Endocrinol Metab*. 2010;299(4):E607–E614.
38. **Yu J, Zhao L, Wang A, et al.** Growth hormone stimulates transcription of the fibroblast growth factor 21 gene in the liver through the signal transducer and activator of transcription 5. *Endocrinology*. 2012;153(2):750–758.
39. **Chen W, Hoo RL, Konishi M, et al.** Growth hormone induces hepatic production of fibroblast growth factor 21 through a mechanism dependent on lipolysis in adipocytes. *J Biol Chem*. 2011; 286(40):34559–34566.
40. **Inagaki T, Lin VY, Goetz R, Mohammadi M, Mangelsdorf DJ, Kliewer SA.** Inhibition of growth hormone signaling by the fasting-induced hormone FGF21. *Cell Metab*. 2008;8(1):77–83.
41. **Owen BM, Bookout AL, Ding X, et al.** FGF21 contributes to neuroendocrine control of female reproduction. *Nat Med*. 2013;19(9): 1153–1156.
42. **Tong X, Muchnik M, Chen Z, et al.** Transcriptional repressor E4-binding protein 4 (E4BP4) regulates metabolic hormone fibroblast growth factor 21 (FGF21) during circadian cycles and feeding. *J Biol Chem*. 2010;285(47):36401–36409.
43. **Durovcova V, Marek J, Hana V, et al.** Plasma concentrations of fibroblast growth factors 21 and 19 in patients with Cushing's syndrome. *Physiol Res*. 2010;59(3):415–422.
44. **Laskewitz AJ, van Dijk TH, Bloks VW, et al.** Chronic prednisolone treatment reduces hepatic insulin sensitivity while perturbing the fed-to-fasting transition in mice. *Endocrinology*. 2010;151(5): 2171–2178.
45. **Yu H, Xia F, Lam KS, et al.** Circadian rhythm of circulating fibroblast growth factor 21 is related to diurnal changes in fatty acids in humans. *Clin Chem*. 2011;57(5):691–700.
46. **Andersen B, Beck-Nielsen H, Hojlund K.** Plasma FGF21 displays a circadian rhythm during a 72-h fast in healthy female volunteers. *Clin Endocrinol (Oxf)*. 2011;75(4):514–519.
47. **Wildenhoff KE, Johansen JP, Karstoft H, Yde H, Sorensen NS.** Diurnal variations in the concentrations of blood acetoacetate and 3-hydroxybutyrate. The ketone body peak around midnight and its relationship to free fatty acids, glycerol, insulin, growth hormone and glucose in serum and plasma. *Acta Med Scand*. 1974;195(1–2):25–28.
48. **Ohshima K, Shargill NS, Chan TM, Bray GA.** Adrenalectomy reverses insulin resistance in muscle from obese (ob/ob) mice. *Am J Physiol*. 1984;246(2 Pt 1):E193–E197.
49. **Liu Y, Nakagawa Y, Wang Y, et al.** Increased glucocorticoid receptor and 11β-hydroxysteroid dehydrogenase type 1 expression in hepatocytes may contribute to the phenotype of type 2 diabetes in db/db mice. *Diabetes*. 2005;54(1):32–40.
50. **Andrews RC, Rooyackers O, Walker BR.** Effects of the 11 β-hydroxysteroid dehydrogenase inhibitor carbenoxolone on insulin sensitivity in men with type 2 diabetes. *J Clin Endocrinol Metab*. 2003;88(1):285–291.
51. **Torrecilla E, Fernandez-Vazquez G, Vicent D, et al.** Liver upregulation of genes involved in cortisol production and action is associated with metabolic syndrome in morbidly obese patients. *Obes Surg*. 2012;22(3):478–486.
52. **Li H, Fang Q, Gao F, et al.** Fibroblast growth factor 21 levels are increased in nonalcoholic fatty liver disease patients and are correlated with hepatic triglyceride. *J Hepatol*. 2010;53(5):934–940.
53. **Mraz M, Bartlova M, Lacinova Z, et al.** Serum concentrations and tissue expression of a novel endocrine regulator fibroblast growth factor-21 in patients with type 2 diabetes and obesity. *Clin Endocrinol (Oxf)*. 2009;71(3):369–375.
54. **Zhang X, Yeung DC, Karpisek M, et al.** Serum FGF21 levels are increased in obesity and are independently associated with the metabolic syndrome in humans. *Diabetes*. 2008;57(5):1246–1253.